Available online at www.sciencedirect.com
SCIENCE DIRECT
Polymer 46 (2005) 11918–11926
polymer
www.elsevier.com/locate/polymer

Monte Carlo simulation of chain extension using bisoxazolines as coupling agent

Li-Tang Yan, Zhen-Yu Qian, Bao-Hua Guo *, Jun Xu, Xu-Ming Xie *

Advanced Materials Laboratory, Department of Chemical Engineering, Tsinghua University, Beijing 100084, People's Republic of China

Received 21 July 2005; received in revised form 5 October 2005; accepted 7 October 2005
Available online 27 October 2005

Abstract

The chain extension using bisoxazolines (OO) as coupling agent was studied by means of the Monte Carlo (MC) method, focusing on the reaction kinetics. A comparison between simulated results and those calculated by an improved kinetic model was made. The coupling efficiency of the chain extender, average molecular weight and molecular weight distributions (MWDs) were investigated. The results show that the biggest coupling efficiency, the highest average molecular weight and the narrowest MWDs can be obtained when the initial concentrations of carboxyl and oxazoline groups are equal. The results indicate that higher activity difference between the oxazoline group in OO and that in blocked CA can lead to higher average molecular weight and narrower MWDs. Those results are in good agreement with the experiments. Besides above factors, diffusion effect and degradation effect are important factors for the average molecule weight and MWDs. And lower reaction kinetics constants of diffusion effect and degradation effect both result in a higher number-average molecular weight ($\bar{M}_n$). The results also indicate that two peaks, at the different molecular weight, appear in the curve of molecular weight distributions during chain extension reaction. The variation of these two peaks corresponds to different polydispersities.

Keywords: Chain extension; Monte Carlo simulation; Kinetics

1. Introduction

For the production of high tenacity and toughness, industrial yarns and the resin grades suitable for high-performance application, it is necessary to have high molecular weight polymers since high chain length contributes to high toughness and melt viscosity [1,2]. However, it is often difficult to achieve these polymers in conventional batch reactors since the reaction rate is slow and, the presence of some undesired side reactions is not avoided. An alternative approach would be chain extension in the melt-phase via the reaction of the hydroxyl, amino or carboxyl terminals with chain extender and, such chain coupling leads to higher molar mass polymers [3–8]. In principle, these chain extenders must be bifunctional, thermally stable and capable of fast reaction with polymer chain terminals under normal extruder process conditions. For example, OO has proved to be an effective chain extender to couple carboxyl terminals of linear polyesters through addition reaction [3–6]. Some important results related to this topic have been achieved in the past decades [3–13]. For instance, Chalamet et al. [9] proposed a differential equation kinetic model to analyze the experimental condition effects on the reaction conversion and the structure of the polymers. However, these models did not include any particular side reaction such as component degradation and diffusion effect in the high viscous melt, which can actually affect the reaction conversion and, the coupling efficiency of the chain extenders [7,9,35]. It is difficult to obtain the detail information about the average molecular weight, the MWDs and, their relations with reaction conditions and side reactions by these models. Moreover, the precise kinetics of the chain extension reaction has not been completely clear up to now.

On the other hand, it is known that MC simulation has proved to be a powerful tool in the study of both polymer physics and polymer chemistry. This powerful method has been extensively used to study living free-radical polymerization [14], free-radical polymerization [15–17,36], emulsion polymerization [18–20], and so on [21–29,37,38].These simulations have given a greater insight into reactive kinetics, complex molecular processes, gel formation, chain grafting reaction, etc. Recently, Sheng et al. [30] have employed the MC method to investigate the influence of entanglement on

* Corresponding authors. Tel.: +86 10 627 84550; fax: +86 10 627 70304.
E-mail addresses: bhguo@mail.tsinghua.edu.cn (B.-H. Guo), xxm-dce@mail.tsinghua.edu.cn (X.-M. Xie).

0032-3861/$ - see front matter © 2005 Elsevier Ltd. All rights reserved.
doi:10.1016/j.polymer.2005.10.037

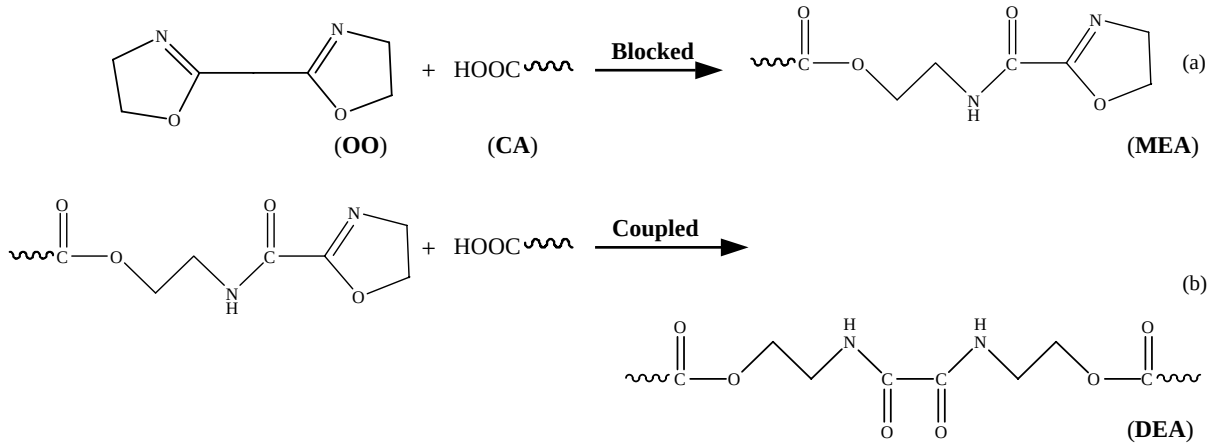

Scheme 1. The scheme of chain extension reactions using a bisoxazoline coupling agent.

the reversible intrachain reaction. The result reveals that biopolymer may utilize the knotting to control the intrachain reaction. However, to the best of our knowledge, the chain extension has not been studied by simulation technique so far.

In the present study, MC method is employed to study the chain extension reaction using OO as coupling agent. The purposes are to give more detail of the chain extension reaction kinetics including the component degradation and diffusion effect and, to exhibit the variation of average molecular weight and MWDs during the reaction.

2. Models and Monte Carlo algorithm

2.1. Modeling

The elementary reactions of carboxyl-terminated polymers (CA) with OO are given in Scheme 1.

The oxazoline groups can react with the carboxyl terminal groups through addition reactions. These reactions lead first to monesteramide (MEA) then to diesteramide (DEA). Reaction behavior of carboxyl terminals contained in the initial polymers can be classified into three groups which are 'blocked', 'coupled' and 'unreacted', respectively. However, these elementary reactions do not include degradation and diffusion effect which can affect the chain extension efficiency especially under extrusion conditions [7,9,35]. After considering these effect factors, the entire reactions are given in Scheme 2.

In Scheme 2, CA(i) is a CA chain with chain length i, MEA(i) is a monesteramide with chain length i, DEA(i) is a diesteramide with chain length i, and ME(i') is a degradation chain with chain length i'. The addition of CA to the first oxaline function of OO can change the reactivity of the residual oxaline, leading to different values for the kinetic constant k_1 and k_2 [9]. Diffusion-controlled effects are important when the reaction involves two large macromolecules [39]. Therefore, in Scheme 2, the diffusion effects of the coupling reaction, i.e. Scheme 2(II), should be considered. A higher diffusion effect corresponds to a slower reaction rate [40,41]. The final results are equivalent to what an imaginary reverse reaction is. So, in this paper, the reverse reaction of the coupling reaction is proposed to consider the diffusion effects. And, for simplicity, each chain is set the same diffusion ability no matter with its chain length. The detailed simulated results including the chain length dependence will be written in our next paper that will be submitted soon [42]. The kinetic constant of Scheme 2(III), k_3, indicates the degree of the diffusion effect. k_4 is the kinetic constant of the degradation reaction of DEA. And the decomposition of DEA is random.

2.2. Monte Carlo algorithm

The principle for the simulation of chain extension was based on the Gillespie's algorithm [31]. A small part of the overall reaction volume is picked out to be a suitable simulation space, which provides most of the information. Suppose the volume V contains a spatially homogeneous mixture of N chemical species, which can interact through S specified chemical reaction channels. The kind of reaction μ that will happen in a time interval $(t+\tau \rightarrow t+\tau+\Delta\tau)$ is determined by a unit-interval uniformly distributed random, r_1, according to the following relation:

$$\mathrm{OO} + \mathrm{CA}(i) \xrightarrow{k_1} \mathrm{MEA}(i) \qquad i = 1, 2, \ldots, i_{\max} \quad \text{Blocking reaction} \qquad \text{(I)}$$

$$\mathrm{MEA}(i) + \mathrm{CA}(j) \xrightarrow{k_2} \mathrm{DEA}(i+j) \qquad j = 1, 2, \ldots, j_{\max} \quad \text{Coupling reaction} \qquad \text{(II)}$$

$$\mathrm{DEA}(i+j) \xrightarrow{k_3} \mathrm{MEA}(i) + \mathrm{CA}(j) \quad \text{or} \quad \mathrm{MEA}(j) + \mathrm{CA}(i) \quad \text{Diffusion effect} \qquad \text{(III)}$$

$$\mathrm{DEA}(i+j) \xrightarrow{k_4} \mathrm{ME}(i) + \mathrm{ME}(j) \qquad \text{Degradation of products} \qquad \text{(IV)}$$

Scheme 2. The entire chain extension concerned in the simulation.

$$\sum_{v=1}^{\mu-1} R_v < r_1 \sum_{v=1}^{S} R_v < \sum_{v=1}^{\mu} R_v \tag{1}$$

where R_v is the rate of vth reaction per molecule in the simulation volume. The time interval between two successive reaction, τ, is a stochastic variable determined by a unit-interval, uniformly distributed random number, r_2,

$$\tau = \frac{1}{\sum_{v=1}^{S} R_v} \ln\left(\frac{1}{r_2}\right) \tag{2}$$

In the present study, the rates from reaction (1)–(4) are listed as follows.

$$R_1 = k_1^{\mathrm{MC}}[\mathrm{OO}][\mathrm{CA}] \tag{3}$$

$$R_2 = k_2^{\mathrm{MC}}[\mathrm{MEA}][\mathrm{CA}]$$

$$R_3 = k_3^{\mathrm{MC}}[\mathrm{DEA}]$$

$$R_4 = k_4^{\mathrm{MC}}[\mathrm{DEA}]$$

where [OO], [CA], [MEA], and [DEA] are the concentrations of OO, CA, MEA and DEA, respectively.

As the microscopic elementary reactions occurred in the simulation, the kind of the reaction that took place in a time interval $(t+\tau \rightarrow t+\tau+\Delta\tau)$ could be determined by the probability of each reaction. The following relationship can be obtained:

$$P_v = \frac{R_v}{\sum_{v=1}^{S} R_v} \tag{4}$$

and it satisfies the relation

$$\sum_{v=1}^{S} P_v = 1 \tag{5}$$

The MC rate constant, k^{MC}, is microscopic and can be transformed into the macroscopic experimental constant, k^{exp}, according to the following relationships:

$$k^{\mathrm{MC}} = k^{\mathrm{exp}} \text{ (for first} - \text{order reactions)} \tag{6}$$

$$k^{\mathrm{MC}} = \frac{k^{\mathrm{exp}}}{VN_{\mathrm{A}}} \text{ (for second} - \text{order reactions)} \tag{7}$$

where N_{A} is the Avogadro's constant and V is the total volume of the system. V can be eliminated by the initial molar concentration of one kind of reactant, e.g. $[\mathrm{B}]_0$, through the definition of molar concentration, $VN_{\mathrm{A}} = X_{\mathrm{B}}^0/[\mathrm{B}]_0$, with X_{B}^0 as the initial number of molecules of species B used in MC simulation [14,32,33]. Using the above process, the simulated results are given in real time scale and can be directly compared with the experimental results.

This study primarily concerns the use of carboxyl-terminated polyamide12 as a model reactant with OO. A total of 20,000 CA chains were initially generated in this simulation. The MWDs of these chains is shown in Fig. 1. The main simulated reaction temperature was 200 °C. The kinetic constant k_1 was obtained

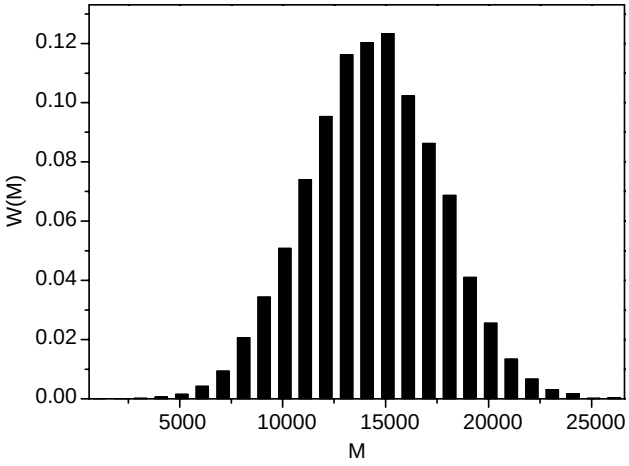

Fig. 1. MWDs of initial 20,000 CA chains.

from the calculation according to the corresponding rate constant at lower temperature and activation energies. The reaction activities of different oxazoline groups change with their molecular structures, leading to different values of the reaction rate constants. Moreover, the variations of these kinetic constants, within appropriate ranges, can be used to investigate the degrees of relative effect factors. So, based on the value of k_1, different values of other kinetic constants, including k_2, k_3 and k_4, were selected. For k_1, a value of 2×10^{-4} kg mol^{-1} s^{-1} at 120 °C with the activation 79.5 kJ mol^{-1} was reported in Ref. [9]. Using the Arrhenius equation, a value of 1.03×10^{-2} kg mol^{-1} s^{-1} was obtained. The initial concentration of carboxyl group, $[\mathrm{COOH}]_0$, was set 1 mmol g^{-1}. And the variational initial concentrations of OO, $[\mathrm{OO}]_0$, were selected to exact the effect of functional group ratio on the chain extension reaction. The reaction is considered to be completed when the conversions of all species are unchangeable. In the following section, it can be found that those values result in a good agreement with the experimental data.

2.3. Amendment for the Chalamet–Taha's kinetic model

The Chalamet–Taha's kinetic model dose not include degradation and diffusion effect [9]. In order to compare the results simulated by MC with those calculated by the differential equation model, the model is modified in this section. Base on the Scheme 2, the evolutions of the different species of the system are:

$$\frac{\mathrm{d}[\mathrm{OO}]}{\mathrm{d}t} = -2k_1[\mathrm{CA}][\mathrm{OO}] \tag{8}$$

$$\frac{\mathrm{d}[\mathrm{CA}]}{\mathrm{d}t} = -[\mathrm{CA}][2k_1[\mathrm{OO}] + k_2[\mathrm{MEA}]] + k_3[\mathrm{DEA}] \tag{9}$$

$$\frac{\mathrm{d}[\mathrm{MEA}]}{\mathrm{d}t} = [\mathrm{CA}][2k_1[\mathrm{OO}] - k_2[\mathrm{MEA}]] + k_3[\mathrm{DEA}] \tag{10}$$

$$\frac{\mathrm{d}[\mathrm{DEA}]}{\mathrm{d}t} = k_2[\mathrm{CA}][\mathrm{MEA}] - k_3[\mathrm{DEA}] - k_4[\mathrm{DEA}] \tag{11}$$

$$\frac{d[ME]}{dt} = 2k_4[DEA] \tag{12}$$

For simplicity, the final normalized differential equations are given directly as follow:

$$\frac{dX}{dt} = -2K_1AX \tag{13}$$

$$\frac{dA}{dt} = -rK_1AX - K_2A[A - 1 + r(1 - X)] + K_3Z \tag{14}$$

$$\frac{dZ}{dt} = K_2[A - 1 + r(1 - X)] - K_3Z - K_4Z \tag{15}$$

$$\frac{dM}{dt} = 2K_4[Z] \tag{16}$$

$$Y = A - 1 + r(1 - X) \tag{17}$$

where $X=[OO]_t/[OO]_{t=0}$, $A=[CA]_t/[CA]_{t=0}$, $Y=[MEA]_t/[CA]_{t=0}$, $Z=[DEA]_t/[CA]_{t=0}$, $M=[ME]_t/[CA]_{t=0}$, and $K_i=k_i[PA]_{t=0}$ with $i=1, 2, 3, 4$. r is the stoichiometric ratio and can be defined as

$$r = \frac{[O]_{t=0}}{[CA]_{t=0}} = \frac{2[OO]_{t=0}}{[CA]_{t=0}} \tag{18}$$

where [O] is the concentration of oxazoline groups. The detail deduction on normalized differential equations can refer to Refs. [9] and [34]. The differential equations can be solved by Runge–Kutta method using the same initial conditions as those of MC simulation.

3. Results and discussions

We would first like to compare the simulated results with those obtained from the experiment. Chalamet et al. [9] reported the studies of chain extension reaction between OO and carboxyl terminated polyamide. The molar ratio of oxazoline groups to carboxyl acid groups, r, is 0.66.The reaction temperature is 120 °C. Degradation and diffusion effect are not considered in the simulated system because the experiment was carried out in a very diluted solution and under the reliable experimental conditions. Fig. 2 illustrates the plots of the normalized concentrations of different reactants and resultants against reaction time. The simulated results are highly in agreement with the experimental results. This agreement implies that stochastic simulation can apply to chain extension and the kinetic constant values used in the study are reasonable.

Fig. 3 demonstrates the plots of the normalized concentrations of different reactants and resultants against reaction time. A close relation between the data calculated by the improved Chalamet–Taha's kinetic model and that by the MC simulation is observed. This is a direct proof that the method used to deal with the system is reasonable. Compared to the MC method, the kinetic model is a more straightforward approach. And it is difficult to obtain the detail information about the average molecular weight, the MWDs and, their

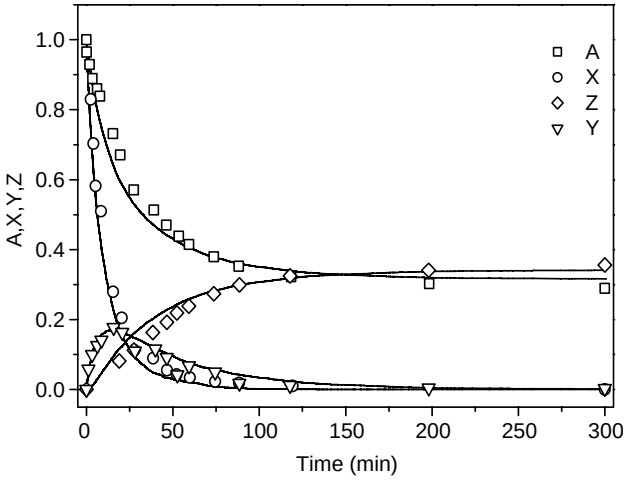

Fig. 2. Dependence of the concentration of different polymers vs reaction time for the chain extension between bisoxazolines and carboxyl-terminated polymers at 120 °C. Parameters used in the simulation are $k_1=k_2=2\times10^{-4}$ kg mol^{-1} s^{-1}, $k_3=k_4=0$ and $r=0.66$.

relations with reaction conditions and side reactions by the kinetic model. However, the kinetic behaviors of chain extension reaction and the change of some parameters, such as MWDs and average molecular weight, can be obtained simultaneously by the MC simulation. Fig. 3 illustrates that the initial reactants vary considerably with the increasing reaction time up to about 10 min. Thereafter, it is slight variation with increasing reaction time while the change of degradation resultants, M, is very small at these stages. Those change trends are basically consistent with the experimental observation [3–6].

The molar ratio of DEA to the initial carboxyl groups, Z, can be used to compare the coupling efficiency of the chain extenders quantitatively. The bigger value of Z indicates the bigger coupling efficiency. Fig. 4(a)–(d) illustrates

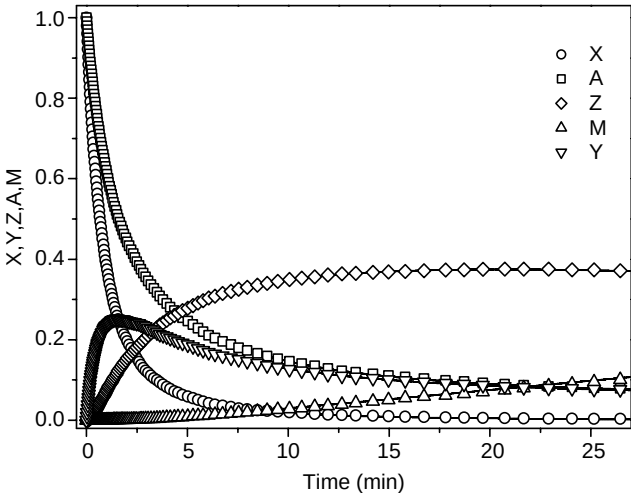

Fig. 3. Plots of the normalized concentrations of different reactants and resultants against reaction time for the chain extension between bisoxazolines and carboxyl-terminated polymers at 200 °C. The dots are the data simulated by MC and solid lines are relative data calculated by the kinetic model. Parameters used in the simulation are $k_1=k_2=1.03\times10^{-2}$ kg mol^{-1} s^{-1}, $k_3=k_4=1.03\times10^{-4}$ s^{-1} and $r=1$.

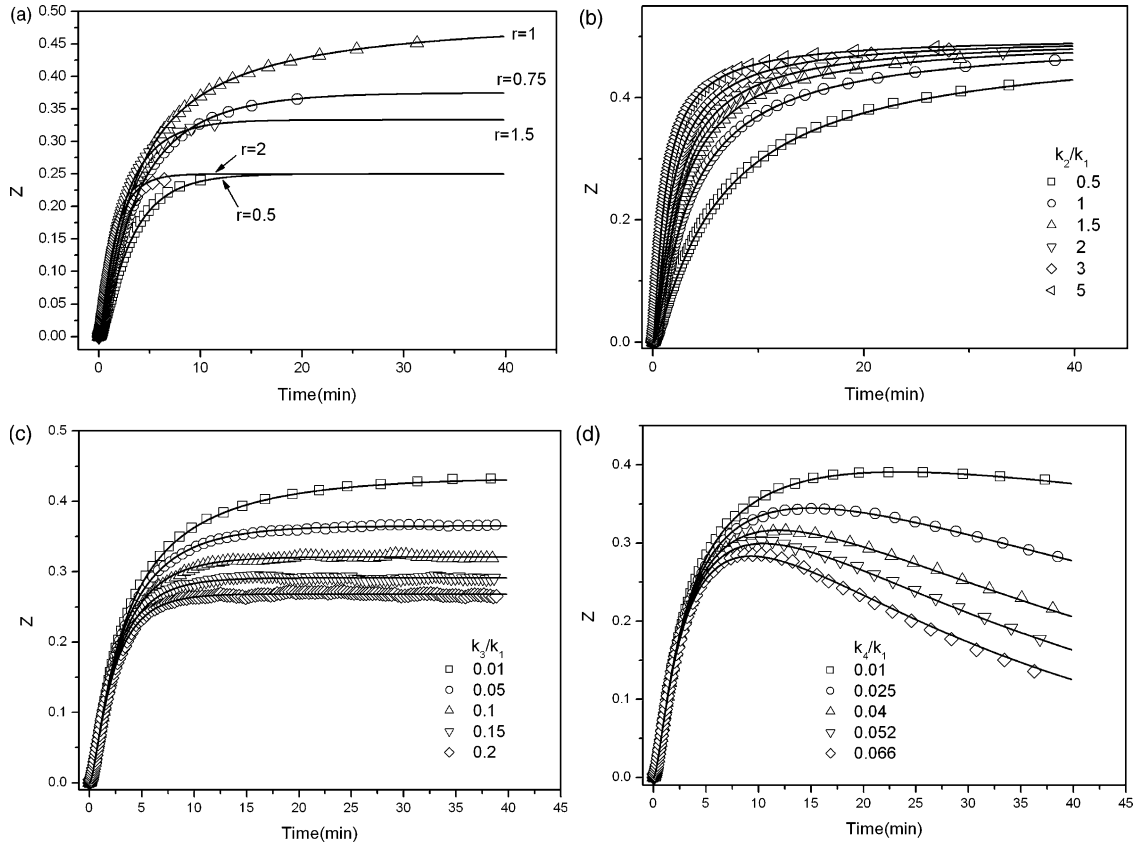

Fig. 4. Plots of molar ratio of DEA to the initial carboxyl groups, Z, against reaction time with different parameters. The dots are the data simulated by MC and solid lines are relative data calculated by the kinetic model. The common parameters used in the simulation are $k_1=1.03\times10^{-2}$ kg mol^{-1} s^{-1}. (a) $k_2=1.03\times10^{-2}$ kg mol^{-1} s^{-1}, $k_3=k_4=0$. (b) $k_3=k_4=0$, $r=1$. (c) $k_2=1.03\times10^{-2}$ kg mol^{-1} s^{-1}, $k_4=0$, $r=1$. (d) $k_2=1.03\times10^{-2}$ kg mol^{-1} s^{-1}, $k_3=0$, $r=1$.

the temporal variation of Z with the change of different parameters. One can found from Fig. 4(a) that the value of Z with $r=1$ is bigger than those of other r at middle and late stages, demonstrating that the coupling efficiency is the highest when the initial concentrations of carboxyl and oxazoline groups are equal. The result is in agreement with the experiment of Inata et al. [4]. The reaction of carboxyl groups to the first oxazoline function of OO can change the reactivity of the residual oxazoline group due to the electron-withdrawing effect, which can lead to different values for the kinetic constant k_1 and k_2 [5]. Fig. 4(b) demonstrates the value of Z increases with the increasing ratio of k_2 to k_1, indicating that the more difference between the oxazoline group in OO and that in blocked CA leads to the bigger coupling efficiency. Fig. 4(c) illustrates the diffusion effect on the coupling efficiency. With the increasing ratio of k_3 to k_1, the value of Z decreases, which demonstrates that the diffusion effect can weaken the effectiveness of the chain extender. The effect of the degradation on the coupling efficiency is shown in Fig. 4(d). It is obvious that the coupling efficiency decreases with the increase of k_4 in the middle and late stages, which is basically consistent with the experiment under the high temperature and in the extrusion condition [35].

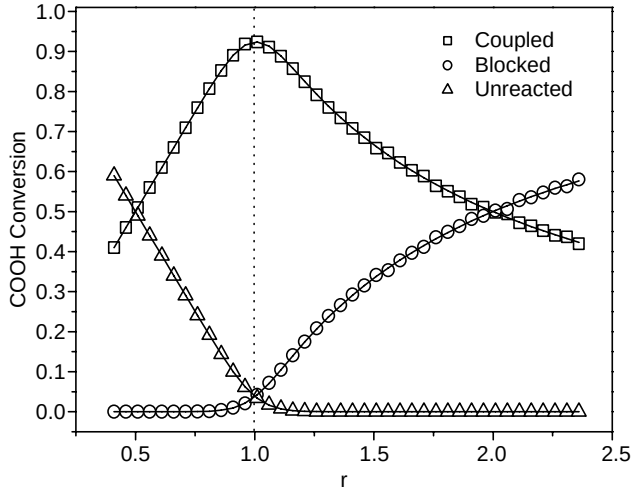

Fig. 5. The relationships between three group polymers and the molar ratio of oxazoline groups to carboxyl acid groups, r. The dots are the data simulated by MC and solid lines are relative data calculated by the kinetic model. Parameters used in the simulation are $k_1=k_2=1.03\times10^{-2}$ kg mol^{-1} s^{-1}, $k_3=k_4=1.03\times10^{-4}$ s^{-1}.

Fig. 5 implies the variations of three group polymers, i.e. 'blocked ', 'coupled ' and 'unreacted', with the change of r after the reactions have adequately reacted. A peak appears at the curve of the coupled group when the concentrations of carboxyl and oxazoline groups are equal, corresponding to the result obtained from Fig. 4(a). The blocked CA is almost unchangeable when r is less than 1. When r is more than 1, the blocked group increases considerably whereas the coupled

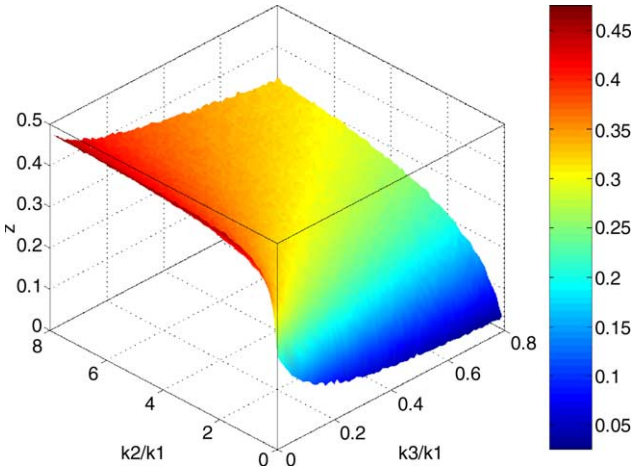

Fig. 6. The final molar ratio of DEA to the initial carboxyl groups, Z, as a function of the kinetic constants k_2 and k_3. Parameters used in the simulation are $k_1=1.03\times10^{-2}$ kg mol^{-1} s^{-1}, $k_4=1.03\times10^{-4}$ s^{-1} and $r=1$.

group decreases with the increasing r, which demonstrate that the excess amount of the chain extender can lead to more blocked groups but lower coupling efficiency.

Fig. 6 is a three-dimensional diagram showing the relationship among the molar ratio of DEA to the initial carboxyl groups, Z, the kinetic constant k_2 and k_3. The reactions have adequately reacted in this simulation. It can be found from Fig. 6 that the variational scope of Z becomes bigger and bigger with the increasing k_3. This demonstrates that the diffusion effect can considerably change the effect of the activity difference between the oxazoline group in OO and that in blocked CA. In other words, the final coupled efficiency is determined by these complicated factors.

Besides coupling efficiency, the average molecular weight and MWDs are important characters of the chain extension. Fig. 7(a)–(d) illustrates the temporal variations of $\bar{M}_n$ with the change of different parameters. The insets are the relative variations of the polydispersity index, d. The variations of $\bar{M}_n$ are basically consistent with those of coupled efficiency (Fig. 4). The inset of Fig. 7(a) shows that the polydisperity index, d, markedly increases at the initial stage. However, in the metaphase and later stages, the decensive scope of d varies with r. The values of d with $r=1$ are the smallest, which demonstrates that, when the chain extender is added in an equal molar amount of the carboxyl terminals, the final MWDs is the narrowest. Fig. 7(b) implies that a peak appears in each curve of d. And the peaks shift in the earlier stage with the increasing ratio of k_2 to k_1, indicating that the final MWDs becomes narrower when the activity difference between the oxazoline group in OO and that in blocked CA becomes bigger. Polydisperity index, d, increases extremely at the initial stage in Fig. 7(c). Then d decreases with the increasing time and, the descensive scope increases with the increasing k_3. This indicates that the final MWDs becomes wider with the stronger

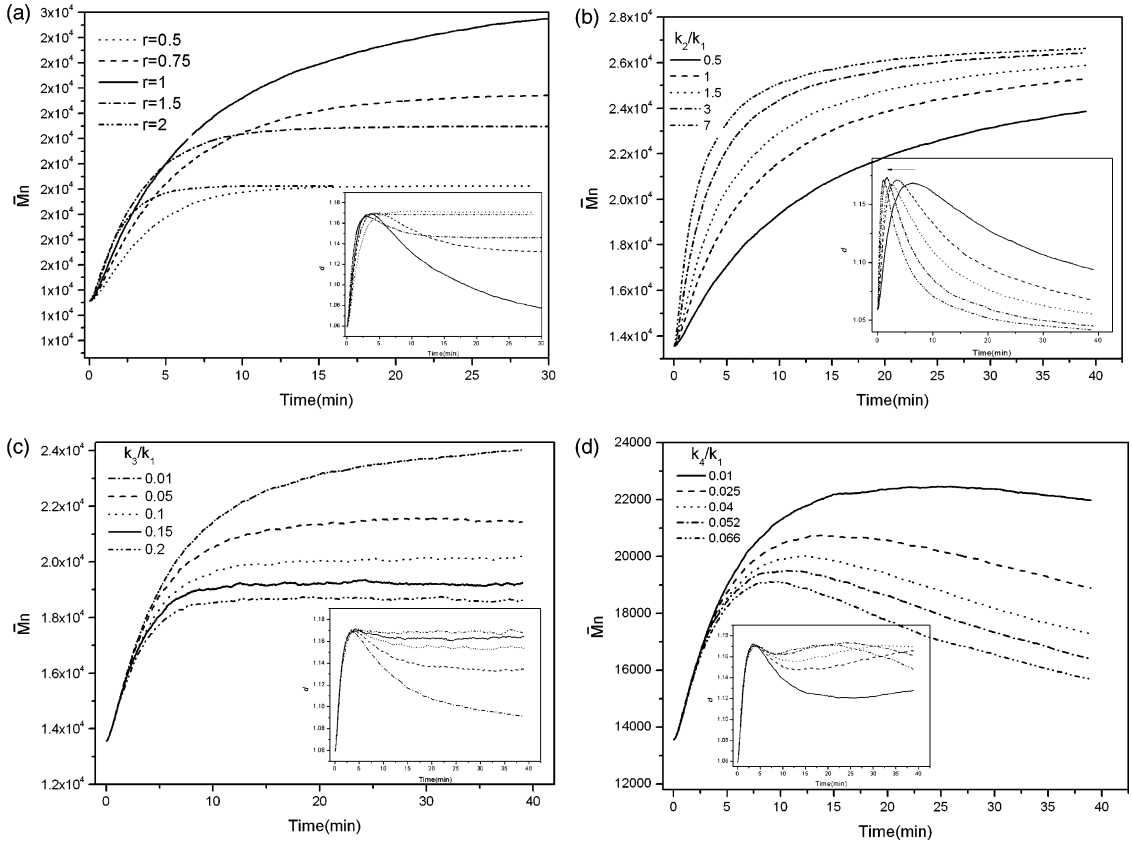

Fig. 7. Plots of the number-average molecular weight, $\bar{M}_n$, against reaction time with different parameters. The insets are the relative variations of the polydispersity index, d. The common parameters used in the simulation are $k_1=1.03\times10^{-2}$ kg mol^{-1} s^{-1}. (a) $k_2=1.03\times10^{-2}$ kg mol^{-1} s^{-1}, $k_3=k_4=0$. (b) $k_3=k_4=0$, $r=1$. (c) $k_2=1.03\times10^{-2}$ kg mol^{-1} s^{-1}, $k_4=0$, $r=1$. (d) $k_2=1.03\times10^{-2}$ kg mol^{-1} s^{-1}, $k_3=0$, $r=1$.

diffusion effect. The inset of Fig. 7(d) illustrates that the change of d is disorder at the last stage, which is due to the random degradation of the resultant.

Fig. 8 exhibits the relationship among $\bar{M}_n$, the change of r and the ratio of k_2 to k_1. The chain extension reactions have adequately reacted. A peak appears in the surface with $r=1$. And the value of the peak becomes bigger and bigger with the increasing ratio of k_2 to k_1. The variation of $\bar{M}_n$ with the change of r corresponds to that of the coupling efficiency in Fig. 5. $\bar{M}_n$ increases with the increasing ratio of k_2 to k_1, indicating that the higher activity difference between the oxazoline group in OO and that in blocked CA can lead to the higher average molecular weight. Fig. 9 is a three-dimensional diagram showing the variation of $\bar{M}_n$ with the change of k_3 and k_4. The plot shows that a lower k_3 and a lower k_4 both result in a higher $\bar{M}_n$. Therefore, besides the molar ratio of oxazoline groups to carboxyl groups and activity difference between the oxazoline group in OO and that in blocked CA, degradation and diffusion effect are important factors for the average molecule weight in chain extension.

Fig. 10 gives the plots of normalized weight-average molecule weight ($\bar{M}_w$), $\bar{M}_n$ and polydispersity index, d, against the conversation of the carboxyl groups, p. The solid lines are calculated by the model as follow [34]

$$\frac{M_{n,t}}{M_{n,0}} = \frac{1+r}{1+r(1-p)} \tag{19}$$

$$\frac{M_{w,t}}{M_{w,0}} = 1 + \frac{2rp}{(1+r)} \tag{20}$$

It is seen that the simulated results are very similar with those calculated by the model. However, this model does not consider the MWDs, which leads to the discrimination between the simulated and calculated results when p is larger. The figure indicates that, with the increasing conversation of the carboxyl groups, there is a peak in the curve of the polydispersity index,

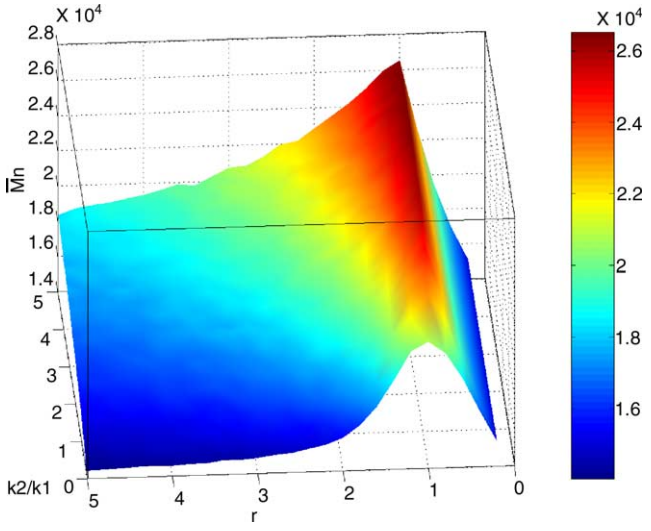

Fig. 8. The relationship among the final number-average molecule weight, $\bar{M}_n$, r and the ratio of the kinetic constants k_2 to k_1. Parameters used in the simulation are $k_1=1.03\times10^{-2}$ kg mol^{-1} s^{-1}, $k_3=k_4=1.03\times10^{-4}$ s^{-1}.

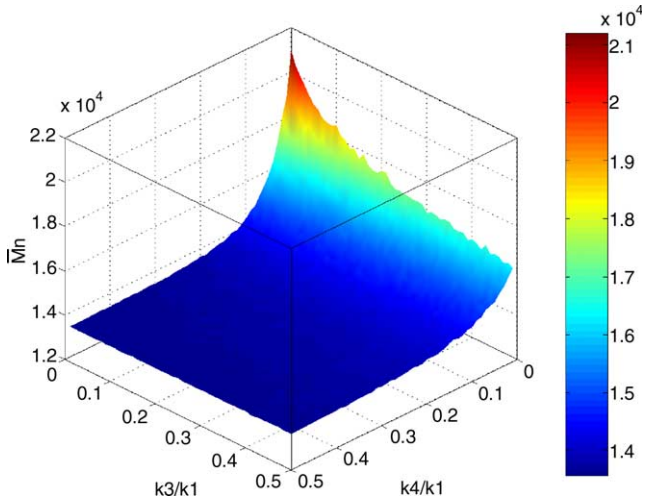

Fig. 9. The relationship among the final number-average molecule weight, $\bar{M}_n$, k_3/k_1 and k_4/k_1. Parameters used in the simulation are $k_1=k_2=1.03\times10^{-2}$ kg mol^{-1} s^{-1} and $r=1$.

demonstrating that the MWDs in the middle stage is wider than those in the initial and last stages.

Fig. 11 illustrates the changes of the MWDs with the reaction time. With the increasing reaction time, a new peak appears at the high molecular weight and becomes higher and higher, meanwhile, the original peak becomes lower and lower till almost disappear at the long reaction time. The simulated result is basically consistent with the experimental results made by Inata et al. [6]. There is only one peak in the initial stage and later stages while two peaks coexist at the middle stage of reaction process. So the MWDs in the middle stage is wider than those in the initial and last stages, corresponding to the simulated results of the polydispersity index, d.

Fig. 12(a)–(d) exhibits plots of the final MWDs with the change of different parameters. The reactions have adequately reacted in this simulation. It can be found from Fig. 12(a) that there is only one peak with $r=1$ while two peaks with the other

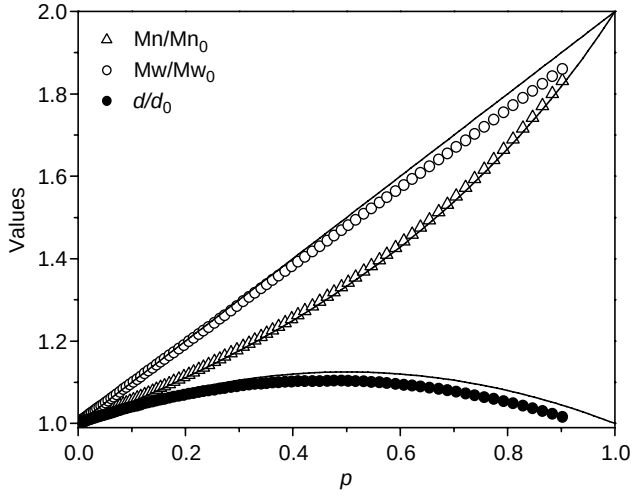

Fig. 10. Plots of normalized $\bar{M}_w$, $\bar{M}_n$, and polydispersity index, d, against the conversation of the carboxyl groups, p. The dots are the data simulated by MC and solid lines are relative data calculated by a model. Parameters used in the simulation are $k_1=k_2=1.03\times10^{-2}$ kg mol^{-1} s^{-1}, $k_3=k_4=0$ and $r=1$.

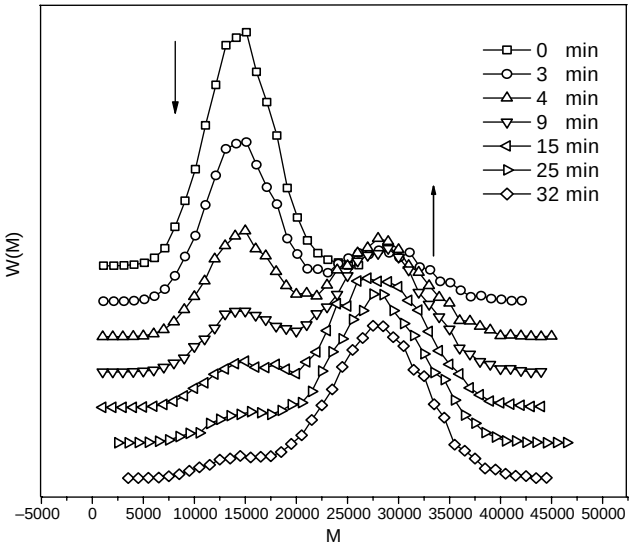

Fig. 11. Plots of the MWDs with the reaction time. Parameters used in the simulation are $k_1=k_2=1.03\times10^{-2}$ kg mol^{-1} s^{-1}, $k_3=k_4=0$ and $r=1$.

values of r. So the MWDs is the narrowest when the functional groups are equal, corresponding to the simulated results of polydispersity index and coupling efficiency. Fig. 12(b) illustrates that the peak at the smaller molecule weight is much lower than that at the higher molecule weight when k_2/k_1 is small and, disappears with the increasing k_2/k_1, indicating that the MWDs becomes narrower with more difference between the oxazoline group in OO and that in blocked CA, which is also in agreement with the simulated results of polydispersity index and coupling efficiency. Fig. 12(c) indicates that the peak at small molecule weight becomes higher while the peak at the high molecule weight becomes lower with the increasing k_3/k_1, demonstrating that diffusion effect can weaken the process of the chain extension. Fig. 12(d) implies the degradation effect on the MWDs. It demonstraters that that the peak at the small molecule weight becomes higher while the peak at the high molecule weight becomes lower with the increasing k_4/k_1, which is basically consistent with the simulated result of coupling efficiency.

4. Conclusions

Monte Carlo simulation was successfully used to investigate the chain extension reaction using bisoxazolines as coupling agent. The results show that bigger coupling efficiency, higher average molecular weight and narrower MWDs can be obtained when the initial concentrations of carboxyl and oxazoline groups are equal. The bigger activity difference

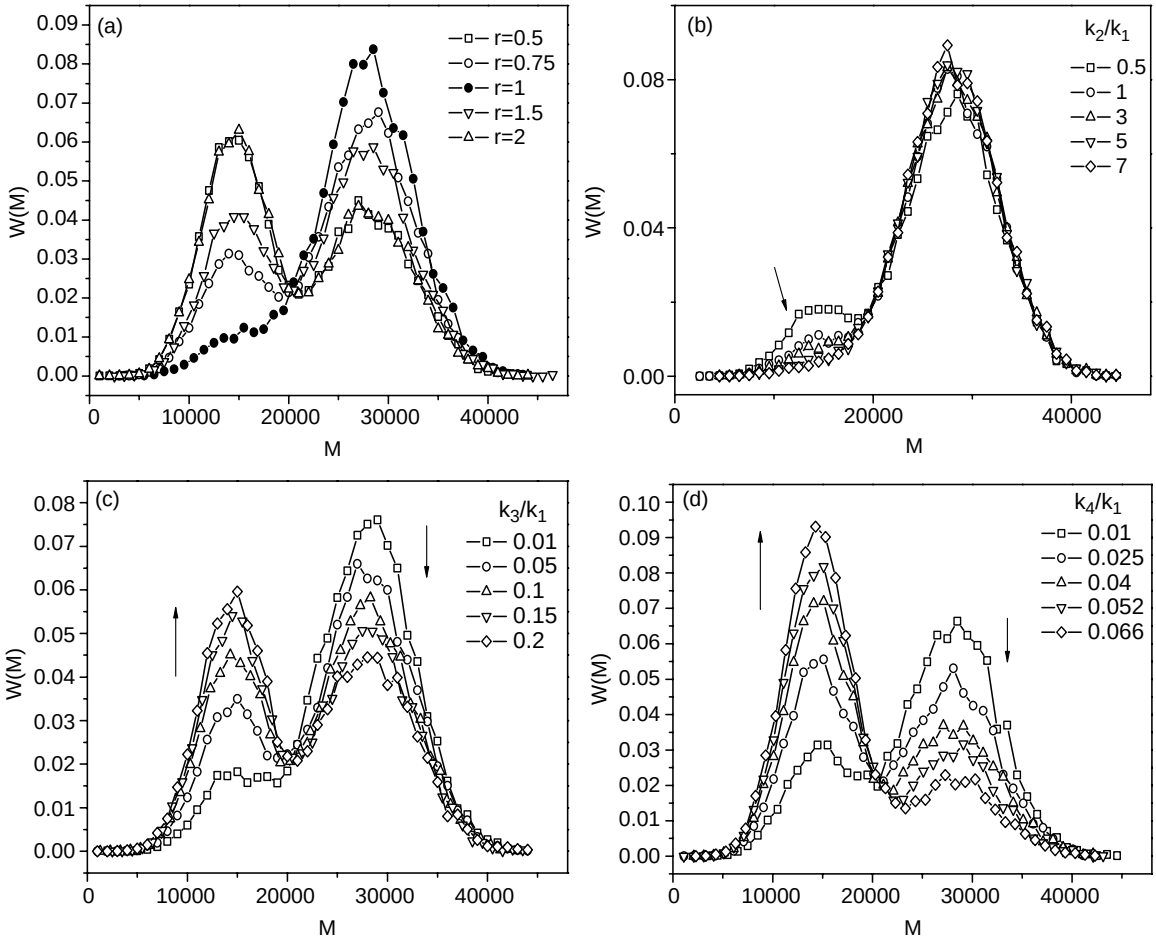

Fig. 12. Relationship between final MWDs and different parameters. The common parameters used in the simulation are $k_1=1.03\times10^{-2}$ kg mol^{-1} s^{-1}. (a) $k_2=1.03\times10^{-2}$ kg mol^{-1} s^{-1}, $k_3=k_4=0$. (b) $k_3=k_4=0$, $r=1$. (c) $k_2=1.03\times10^{-2}$ kg mol^{-1} s^{-1}, $k_4=0$, $r=1$. (d) $k_2=1.03\times10^{-2}$ kg mol^{-1} s^{-1}, $k_3=0$, $r=1$.

between the oxazoline group in OO and that in blocked CA can lead to higher average molecular weight and narrower MWDs. Those results are in agreement with the experiments. Besides the molar ratio of oxazoline groups to carboxyl groups and activity difference between the oxazoline group in OO and that in blocked CA, degradation and diffusion effect are important factors for the average molecule weight and MWDs. And a lower k_3 and a lower k_4 both result in a higher $\bar{M}_n$. The results also indicate that two peaks, at the different molecular weight, appear in the curve of molecular weight distributions during chain extension reaction. And the variation of these two peaks corresponds to different polydispersities. The MWDs in the middle stage is wider than those in the initial and last stages.

Acknowledgements

Financial support from the National Natural Science Foundation of China (No. 50043016, No. 90103035, No. 20174022 and No. 10334020) and the Specialized Research Fund for the Doctoral Program of Higher Education (No. 20040003033) is highly appreciated.

References

[1] Paul DR, Newman S. Polymer blends. vols. 1 and 2. New York: Academic; 1976.
[2] Xanthos M. Reactive extrusion. Munich: Brown SB Inc.; 1992.
[3] Inata H, Matsumura S. J Appl Polym Sci 1985;30:3325–37.
[4] Inata H, Matsumura S. J Appl Polym Sci 1986;32:5193–202.
[5] Inata H, Matsumura S. J Appl Polym Sci 1986;32:4581–94.
[6] Inata H, Matsumura S. J Appl Polym Sci 1987;34:2769–76.
[7] Akkapeddi MK, Gervasi J. Polym Prepr 1988;29:567–70.
[8] Loontjens T, Belt W, Stanssens D, Weerts P. Polym Bull 1993;30:13–18.
[9] Chalamet W, Taha M. J Polym Sci, Polym Chem Ed 1997;35:3697–705.
[10] Chalamet W, Taha M. J Appl Polym Sci 1999;74:1017–24.
[11] Douhi A, Fradet A. J Polym Sci, Polym Chem Ed 1995;33:691–9.
[12] Acevedo M, Fradet A. J Polym Sci, Polym Chem Ed 1993;31:817–30.
[13] Acevedo M, Fradet A. J Polym Sci, Polym Chem Ed 1993;31:1579–88.
[14] He J, Zhang H, Chen J, Yang Y. Macromolecules 1997;30:8010–8.
[15] Tobita H. Macromolecules 1993;26:836–41.
[16] Tobita H. Macromolecules 1995;28:5119–27.
[17] Tobita H. Macromolecules 1997;30:1693–700.
[18] Tobita H, Yamamoto K. Macromolecules 1994;27:3389–96.
[19] Tobita H, Takada Y, Nomura M. Macromolecules 1994;27:3804–11.
[20] Nie L, Yang W, Zhang H, Fu S. Polymer 2005;46:3175–84.
[21] Chung I. Polymer 2000;41:5643–51.
[22] Cheng K, Chiu W. Macromolecules 1994;27:3406–14.
[23] Klos L, Pakula T. Macromolecules 2004;37:8145–51.
[24] Yan D, Dong H, Ye P, Müller AHE. Macromolecules 1996;29:8057–63.
[25] He C, Costeux S, Wood-Adams P, Dealy JM. Polymer 2003;44:7181–8.
[26] Wolterink JK, Barkema GT, Cohen MAS. Macromolecules 2005;38:2009–14.
[27] He X, Liang H, Pan C. Polymer 2003;44:6697–706.
[28] Cao D, Wu J. Macromolecules 2005;38:971–8.
[29] Zhu Y, An L, Jiang W. Macromolecules 2003;36:3714–20.
[30] Sheng Y, Wu C, Lai P, Tsao H. Macromolecules 2005;38:2959–65.
[31] Gillespie DT. J Phys Chem 1977;81:2340–61.
[32] Lu J, Zhang H, Yang Y. Macromol Theor Simul 1993;2:747–60.
[33] He J, Zhang H, Yang Y. Macromol Theor Simul 1995;4:811–9.
[34] Qian Z-Y, Guo B-H, Shi J-Z, Xu J. Acta Polym Sin 2004;4:506–10.
[35] Qian Z-Y, Guo B-H, Shi J-Z, Xu J. Acta Polym Sin 2004;4:511–7.
[36] Drache M, Schmidt-Naake G, Buback M, Vana P. Polymer 2005;46:8483–93.
[37] Kurt N, Haliloglu T. Polymer 2002;43:403–8.
[38] Carri GA, Batman R, Varshney V, Dirama TE. Polymer 2005;46:3809–17.
[39] Delgadillo-Velázquez O, Vivaldo-Lima E, Quintero-Ortega IA, Zhu S. AIchE J 2002;48:2597–608.
[40] Collins FC, Kimball GE. J Colloid Sci 1949;4:425–37.
[41] Guzmán JD, Pollard R, Schieber JD. Macromolecules 2005;38:188–95.
[42] Yan L-T, Guo B-H, Xu J, Xie X-M. Submitted to Macromolecules.